THERAPSIDS FROM THE PERMIAN CHIWETA BEDS AND THE AGE OF THE KAROO SUPERGROUP IN MALAWI

Louis L. Jacobs, Dale A. Winkler, Kent D. Newman, Elizabeth M. Gomani, and Alan Deino

ABSTRACT

Exposures of the Karoo Supergroup occur in the northern and southern portions of Malawi, south central Africa. The section in southern Malawi contains Lower Permian coal-bearing shales and extends upward to the Chikwawa basalt of Jurassic age (179 Ma). The Chikwawa basalt represents the northern limit of the Karoo Large Igneous Province, which signals the rifting of Gondwana. The Chiweta Beds of northern Malawi contain a Late Permian (*Cistecephalus* Zone; 256-258 Ma) fauna, including the dicynodont *Oudenodon* and a new burnetiamorph biarmosuchian more derived than *Lemurosaurus* and sister to *Proburnetia*, *Burnetia*, and *Bullacephalus*.

Louis L. Jacobs. Department of Geological Sciences, Southern Methodist University, Dallas, Texas 75275, USA. jacobs@mail.smu.edu

Dale A. Winkler. Department of Geological Sciences, Southern Methodist University, Dallas, Texas 75275, USA. dwinkler@mail.smu.edu

Kent D. Newman. Department of Geological Sciences, Southern Methodist University, Dallas, Texas 75275, USA. knewman@mail.smu.edu

Elizabeth M. Gomani. Department of Antiquities, P.O. Box 264, Lilongwe, Malawi. egomani@yahoo.com

Alan Deino. Berkeley Geochronology Center, 2455 Ridge Road, Berkeley, California 94709, USA. al@bgc.org

INTRODUCTION

In 1989, 1990, and 1992, members of a joint Malawi Department of Antiquities-Southern Methodist University field crew investigating the Creta-ceous Dinosaur Beds of northern Malawi made day trips to Permian Karoo Supergroup rocks near Chiweta (Figure 1). Among other specimens collected were three therapsid skulls, two of the dicynodont *Oudenodon* and one of a burnetiamorph biarmosu-
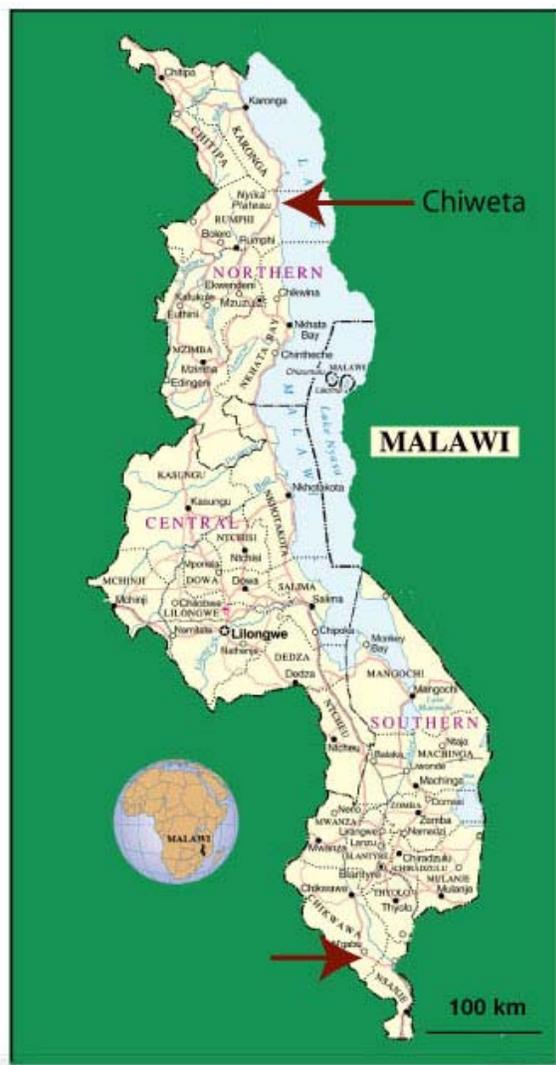
Figure 1. Map of Malawi showing the location of the Chiweta Beds and the location of the Chikwawa basalt where it was sampled for dating near the village of Ngabu.

chian (sensu Sidor and Welman 2003). The burnetiamorph skull was prepared by Will Downs, who was also a member of the field parties in Malawi (Jacobs 1993). He referred to the skull, because of its odd excrescences, as the head of the devil. His enthusiasm for this fossil encouraged us in this study, both to understand the affinity of the specimen, but also for its context and age. The description provided here is based on a cast because the original is not available at this time. The thorough study of the Chiweta Beds and the naming of this new taxon will be overseen by Elizabeth M. Gomani, but we present here an initial description that we hope our friend Will, to whom this paper is dedicated, would appreciate. In addition, we report a radiometric age determination for basalt that

caps the Karoo Chikwawa Group (Habgood 1963) in southern Malawi.

CONTEXT AND HISTORY OF STUDY OF THE MALAWI KAROO

The classic South African Karoo Supergroup (Du Toit 1926) is a suite of Carboniferous to Jurassic sedimentary rocks shed from the Gondwanide Mountains toward lower latitudes, infilling foreland basins, and capped by volcanics generated in conjunction with the rifting of eastern Gondwana (Cox 1970). The Karoo succession begins with Dwyka Group glacial sediments. The Dwyka is followed by the marine and coal-bearing Ecca Group, the richly fossiliferous and mainly fluviatile Beaufort Group, succeeded by the increasingly eolian Stormberg Group, and culminated by the Drakensberg Volcanics (Johnson et al. 1996; Smith et al. 1993).

U/Pb radiometric dates of 302.0 ± 3.0 Ma and 299.2 ± 3.2 Ma were determined from tuffs in the Dwyka Group (as discussed by Stollhofen et al. 2000). In the overlying Ecca Group, dates of 289.6 ± 3.8 Ma and 288.0 ± 3.0 Ma were determined from tuffs in the Prince Albert Formation (Stollhofen et al. 2000). An additional date of 270 ± 1.0 for the Ecca Group was reported from the Collingham Formation (Turner 1999). An absolute age determination of 265 ± 2.5 from the Gai-As Formation, Namibia (Hancox and Rubidge 2001), is correlated with the base of the Beaufort Group. Duncan et al. (1997) reported that Drakensberg Volcanics present highly resolved ages ranging from 184 to 179 Ma, with the majority of dates clustering at 183 ± 1 Ma.

The Carboniferous-Permian boundary falls within the Dwyka Group (Bangert et al. 1999), the Permian-Triassic boundary falls within the Beaufort Group (Hancox et al. 2002), and the Triassic-Jurassic boundary falls within the Elliot Formation of the Stormberg Group (Lucas and Hancox 2001). Increasing aridity and temperature amelioration is indicated throughout the South African succession, due in large part to the northward drift of Gondwana from a near polar 75° South latitude to a low temperate 35° South latitude (Visser 1991), but depositional styles were also influenced by tectonism during the 120 million years of Karoo deposition (Bordy et al. 2004; Smith et al. 1993).

Malawi lies in south central Africa. Its dominant geographic feature is Lake Malawi, a Rift Valley lake and the third deepest lake in the world. Karoo Supergroup rocks are present as fault block outliers in the north and the south of the country. In addition to the therapsid-bearing Chiweta Beds, bone-bearing rocks of Cretaceous age (Dixey

2

1928; Haughton 1928; Jacobs et al. Jacobs et al. 1993) and the Pliocene hominid-bearing Chiwondo Beds (Sandrock et al. 1999; Schrenk et al. 1993) occur in fault grabens located in close proximity to each other along the structurally complex Rift Valley in the north of the country.

The most southerly outcrops of Karoo Supergroup sediments and volcanics in Malawi are referred to as the Chikwawa Group by Habgood (1963; Figure 1) and are preserved in the Shire-Zambezi fault trough between Chikwawa and Chiromo (Habgood 1963). The capping volcanics of the Chikwawa Group extend through the Lupata Gorge area of northern Mozambique to the Lebombo Mountains of southern and western Mozambique and Swaziland, to the Drakensberg Volcanics of Lesotho and South Africa. In southern Malawi, as in northern Mozambique, Cretaceous sediments and volcanics referred to as Lupata Group (Dixie and Smith 1929) overlie Karoo volcanics.

Fragmentary bones identified as "Stormberg dinosaurs" by Sidney Haughton were reported from sediments below the Karoo volcanics in southern Malawi by Dixey (1930). The stratigraphic position of those fossils would suggest a Triassic or Early Jurassic age (Habgood 1963). Karoo volcanics are absent from northern Malawi, and none of the Karoo sediments in the north can be conclusively demonstrated to be younger than Permian. The fossils recovered from the Chiweta Beds are clearly comparable in a biostratigraphic sense to those from the Beaufort Group of the South African Karoo (Rubidge 1995), and as discussed below, indicate a Late Permian age for the Chiweta Beds.

The first bones recognized by Europeans in Karoo rocks of Malawi were fish found in 1883 by Henry Drummond in the far north of the country (Andrew and Bailey 1910; Arber 1910; Drummond 1884, 1888; Jacobs et al. 1992; Jones 1890; Newton 1910; Traquair 1910). The therapsid-bearing Chiweta Beds were visited in 1925 by Frank Dixey during reconnaissance of the area near Livingstonia and south of Mount Chombe (known as Mount Waller in older literature; Dixie 1926; Figure 2). Dixey sent bones from Chiweta to Sidney Haughton in South Africa. Within the sample, Haughton (1926) recognized gorgonopsians, of which he named *Chiwetasaurus dixeyi*, *Dixeya quadrata*, and *Aelurognathus nyasaensis*, and he recognized dicynodonts.

In 1930, not long after Haughton's (1926) publication, F.W.H. Migeod spent two weeks in the Chiweta Beds with F.R. Parrington (Jacobs et al. 1992), and stated that "*Dicynodon* bones were the most common" fossils (Migeod 1931). Collections made by Migeod were shipped to the British Museum (Natural History).

Sigogneau (1970) and Sigogneau-Russell (1989) reviewed the Chiweta gorgonopsians originally reported by Haughton (1926). While noting that there was uncertainty as to generic identity, she transferred the species *Chiwetasaurus dixeyi* to *Gorgonops* with question. Haughton's *Aelurognathus nyasaensis*, while maintained as valid, was considered close to *A. trigriceps*, but Sigogneau-Russell acknowledged that the species was poorly known and might belong to the Rubidgeinae rather than the Gorgonopsinae, where it was originally placed. The genus *Dixeya* was synonymized with *Aelurognathus*, thereby establishing the Chiweta species as *A. quadrata*.

Figure 2. The Chiweta Beds looking to the north. Black and white photo on right is taken from Dixey (1926). Bone-bearing channel and overbank deposits of the Chiweta Beds (B1) are in the foreground. Lake Malawi is in the background. The ridge to the left is composed of older Karoo Supergroup rocks, the valley is floored with lake sediments, which blanket a fault between the down dropped Chiweta Beds and the older Karoo. (See Figure 1 for location.)

STRATIGRAPHY AND AGE
OF THE MALAWI KAROO

The first published stratigraphic section of the Chiweta Beds was that of Dixey (1926). Total thickness of the Karoo was measured to be 1,219 m with the upper 305 m comprising the Chiweta Beds. Later authors have applied a K1-K7 stratigraphic terminology devised for Tanzanian Karoo deposits, with K6 and K7 equivalent to the Chiweta Beds, measured by Cooper and Habgood (1959) to have a thickness of 244 m. Most bones were said to come from the middle of the unit. Gay and Cruickshank (1999) summarized the Tanzanian K6 and K7 units in their table 1 as Alibashian, Late Permian, *Dicynodon* Zone, and Anisian, middle Triassic, *Cynognathus* Zone, respectively. As shown below, these designations are too young as they are applied to the Chiweta Beds.

The Karoo Supergroup of Malawi (Figure 3) exhibits no glacial or marine sediments comparable to the Dwyka Group of South Africa. Coal-bearing strata low in the Karoo section in northern Malawi were correlated with the South African Ecca Group by Cairncross (2001). In southern Malawi, Cairncross (2001) placed the coal shales in the early Tatarian (Late Permian). However, the age of the southern Malawi coal shales is based notably on the presence of the plant species *Gangamopteris obovata* and *Noeggerathiopsis hislopi*, which if correct means these beds may well be Early Permian (Habgood 1963). Given the date of the overlying Chikwawa basalt (see below) and the possible ages of plants in the coal shales, the age range of the southern Malawi Karoo could extend from Early Permian to Jurassic, a longer range than that presented by Cairncross (2001, figure 2; Figure 3).

The Age of the Chikwawa Basalt

The distribution of the Drakensberg Volcanics and related rocks that cap the Karoo Supergroup defines the Karoo Large Igneous Province (LIP). Karoo LIP outcrops extend on the east from the Drakensberg Mountains of South Africa and Lesotho, through the Lebombo Mountains of Swaziland and Mozambique. They include the Etjo basalt of Namibia and the Batoka basalts of Zimbabwe. By proximity to the Lebombo volcanics and the Batoka basalts, the older set of extrusive rocks of the Lupata Gorge in Mozambique (Dixey and Smith 1929), and the Chikwawa basalt of southern Malawi appear to be the northern outcrop limit of the Karoo LIP.

The thickness of the igneous rocks capping the Karoo Chikwawa Group of southern Malawi is
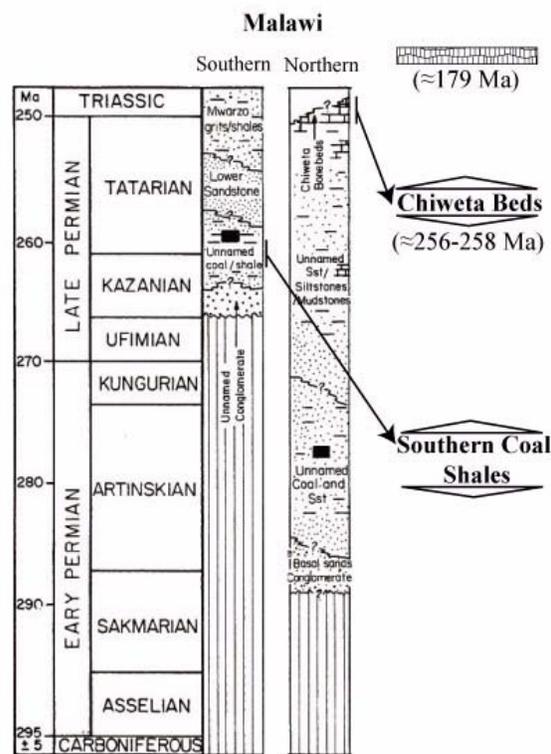
Figure 3. Karoo Supergroup stratigraphic sections from northern and southern Malawi as presented by Cairncross (2001). The right column shows our modifications. The Chikwawa basalt of southern Malawi at 179 Ma is considered to have been emplaced during Karoo LIP magmatism. The Chiweta Beds of northern Malawi are similar in age to the lower portion of the *Cistecephalus* Zone, and the coal shales of southern Malawi are older than reported based on plants. The timescale shown is that used by Cairncross (2001). Gradstein and Ogg (2004) do not recognize Tatarian, but instead use Capitanian, Wuchiapingian, and Changhsingian for the comparable interval. In that scheme, the Chiweta Beds fall within the Wuchiapingian and are estimated to fall between 258 and 256 Mya.

estimated by Habgood (1963) to be 1067 m, but exposures are poor, faulting complicates the relationship of outcrops, and the age is poorly constrained. Nevertheless, as in Karoo extrusives in other areas, weathered surfaces between flows are rare, suggesting a rapid series of eruptions (Habgood 1963). Based on geochronology and paleomagnetism of the Batoka basalts in northern Zimbabwe, Jones et al. (2001) determined that the duration of emplacement of the Karoo LIP was 5 Myr, ranging between approximately 184 to 179 Ma.

We report here the results of laser incremental-heating ^{40}Ar/^{39}Ar age determinations of a Chikwawa basalt flow (sample LJ-4) and a cross-cutting

4

Figure 4. Will Downs at Chikwawa basalt sampling locality near Ngabu, Malawi. (See Figure 1 for location).

basaltic dike (LJ-3) from samples collected in 1990. These rocks are nearly identical, fine-grained intergranular plagioclase and pyroxene basalts showing minor alteration of mineral phases in thin section. The flow overlies Karoo Supergroup sediments on the south side of the Nyakamba River in a roadcut for Highway M8 (Figures 1, 4) near the town of Ngabu (16°27'20"S, 34°43'45"E).

Two aliquots of crushed (0.15 to 0.25 mm) whole rock were analyzed from each of the two samples (Figure 5, see Table 1, Deino et al. 1990, and Sharp et al. 1996, for details of the analytical procedure). Reproducibility of fine details of release patterns in age and geochemical parameters (%^{40}Ar*, Ca/K), and in the derived plateau and integrated ages between aliquots of the same sample, is noteworthy. All spectra released initial fractions (<10% of the cumulative ^{39}Ar release) charged with atmospheric argon and younger than the subsequent plateau, probably reflecting a limited degree of alteration. Nevertheless, broad plateaus occur within the central portion of the release sequence. These plateaus occupy the zone where the Ca/K ratio of the released gasses is less than about 4. In the final 20-30% of the ^{39}Ar release, Ca/K ratios rise sharply and apparent ages fall. This spectral form, characterized by a stair-stepping downward pattern in both the beginning and

end of the incremental-heating sequence, is consistent in all four experiments. It can be interpreted as representing recoil implantation of ^{39}Ar released from fine-grained alteration phases into refractory calcic phases. The fine-grained, ^{39}Ar depleted alteration products release their argon early and exhibit artificially old ages and high atmospheric content, while the ^{39}Ar enriched calcic phases retain their argon to the last, exhibiting young ages and high Ca/K ratios. Despite this redistribution of ^{39}Ar locally, older apparent ages in the early release steps are balanced against young ages in the final steps, so that integrated ages are in all cases congruent with the plateau results.

We take the weighted means of the plateau ages of the replicates as the reference age, and obtain 179.4 ± 0.8 for LJ-3 and 168.6 ± 0.8 for LJ-4. These determinations are clearly distinct and present the apparently inverted age relationship of an older age for the crosscutting basalt than the lava flow it lies within. Either alteration has affected the argon systematics more than is apparent from the spectra and the lava flow is relatively too young, or the dike contains a component of excess argon and is relatively too old.

In either case, these ages are relatively young, but broadly compatible with the emplace-
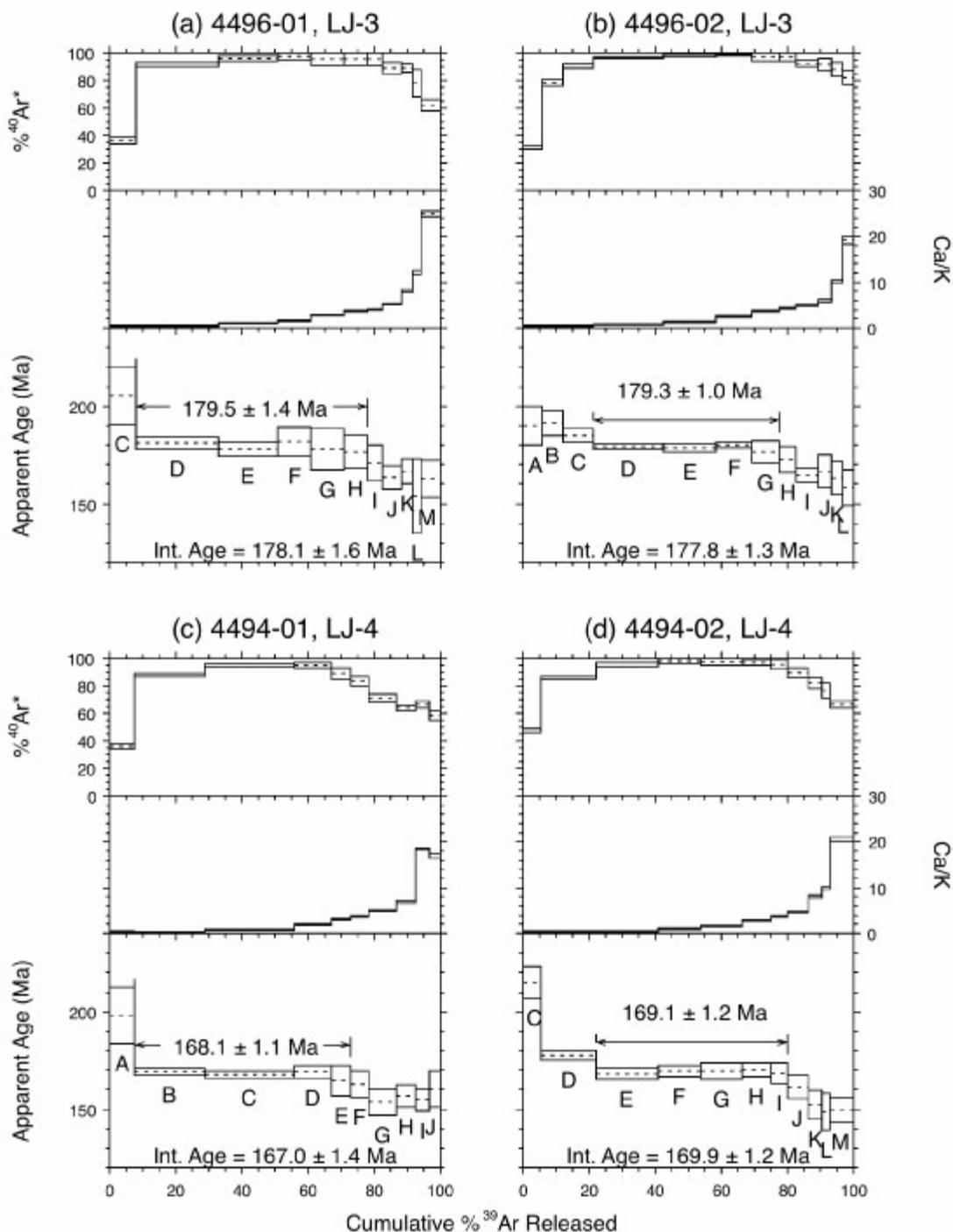
Figure 5. [40]Ar/[39]Ar incremental-heating release spectra of the Chikwawa basalt and cross-cutting dike. '%[40]Ar*' represents the percentage of radiogenic argon released. 'Int. Age' is the integrated age, calculated by isotopic recombination of all experimental steps. 'Plateaus' are formed from those steps that are: 1) contiguous, 2) constitute greater than 50% of the total [39]Ar released, 3) have an acceptable mean square of weighted residuals (MSWD, probability >95%), and 4) not intolerably different from the plateau mean age if an outermost step (>1.4 times the error in age of the step). (A) and (B): Dike cross-cutting Chikwawa basalt, sample LJ-3; (C) and (D), Chikwawa basalt flow, sample LJ-4.

6

Table 1. ^{40}Ar/^{39}Ar incremental-heating values of the Chikwawa basalt and cross-cutting dike sampled near Ngabu, southern Malawi. This table is presented in over-sized format at the end of the chapter.

ment history of the Karoo LIP (184 to 179 Ma, Duncan et al. 1997; Jones et al. 2001). Considering the geographic proximity of the Chikwawa basalt relative to recognized Karoo LIP rocks, the stratigraphic position of the Chikwawa basalt atop Karoo Supergroup sediments, and the age of the lava flow and dike at Ngabu, the Chikwawa basalt is taken to be the northern outcrop extent of the Karoo LIP. The age of the Chikwawa basalt is Jurassic, and in the absence of a major unconformity beneath this flow, the Karoo strata of southern Malawi are much younger than the Triassic age assigned by Cairncross (2001, figure 2; Figure 3).

Northern Malawi

The Chiweta Beds of northern Malawi are fluvial in origin. Bones within overbank deposits are often found encased in pedogenic carbonate, similar to the condition of those from the Beaufort Group of South Africa (Smith 1990, 1993). The most detailed stratigraphic work conducted on the Karoo Supergroup of the Mount Chombe-Chiweta area is that by Yemane et al. (1989), Yemane and Kelts (1990), and Yemane (1993). Approximately 300 m of section were measured, all underlying the therapsid-bearing Chiweta Beds, which were excluded from their studies. Yemane et al (1989) interpreted the environment of deposition to be lacustrine, and while these lacustrine sediments do not preserve bone, they contain pollen (Yemane 1994). Of 20 identified pollen taxa, 15 are unknown after the Permian-Triassic boundary. Eleven of those taxa have records prior to the Late Permian, and four range throughout the Late Permian. Three pollen taxa (*Taeniaesporites noviaulensis*, *Lycopodiacidites pelagius*, and *Rimaesporites aquilonalis*) range only from after the beginning of the Tatarian (late Capitanian or younger *fide* Gradstein and Ogg 2004) and into the Triassic. Therefore, an independent maximum age limit for the overlying Chiweta Beds of <263 Ma (base of the Tatarian, timescale of Gradstein and Ogg 2004) is set from palynological evidence.

Age of the Chiweta Beds Based on Therapsid Biostratigraphy. Dixey (1926) recognized two main bone producing horizons in the Chiweta Beds, although he acknowledged that bone could be found throughout. The main bone producing horizons correspond to his units 5 and 7. Unit 5 is the Lower Bone Bed (or B1), and unit 7 is the

Upper Bone Bed (B2) of Haughton (1926). Our collections were made from the Lower Bone Bed (B1, seen in the foreground in Figure 2) with the possible exception of an articulated but unprepared and unidentified skeleton lacking the skull, which is likely from the Upper Bone Bed (B2).

The upper age limit of the Chiweta Beds can be refined by comparison of the B1 therapsid assemblage with that of the Beaufort Group, the vertebrate biostratigraphy of which is reviewed in Rubidge (1995). Of particular importance is the genus *Oudenodon*, which we show to occur at Chiweta (Figures 6, 7). King diagnosed the Tribe Oudenodontini (which contained only *Oudenodon*) as:

> Medium-sized to large dicynodonts (skull length ranging from 100 mm to over 300 mm). Teeth lacking in both upper and lower jaws. Postorbitals well separated on skull roof by parietals. Septomaxilla recessed within external naris, lachrymal in some species extends forward above maxilla to posterior margin of naris. Nasal forms boss over naris. Maxilla carries weak caniniform process, with sharp edged posterior crest. Palatal portion of palatine divided into inflated posterior area, and a smooth anterior part that meets the premaxilla. Vomers form short septum in anterior part of interpterygoidal fossa. Ectopterygoid large with palatal exposure, pterygoid does not contact maxilla… (King 1988, p. 85).

The characters observed in the dicynodont skulls designated Malawi Department of Antiquities (Mal) 108 and 129 (Figures 6, 7) from the Chiweta Beds indicate that both belong to the genus *Oudenodon*. Mal 108 is lacking its posterior portion. Mal 129 is postdepositionally dorsoventrally compressed. Measurements (Table 2) demonstrate that the two specimens are similar in size and represent a single species, but Mal 129 appears more robust.

Oudenodon groups with *Tropidostoma*, *Rhachiocephalus*, and their most recent common ancestor within a clade (Cryptodontinae) within the Dicynodontidae (sensu King 1988, 1990; Angielczyk 2001; compare Angielczyk and Kurkin 2003a, b). Members of this clade are diagnosed by having a postcaniniform crest. A less inclusive clade within the Cryptodontinae, diagnosed by parietals exposed in a depression between the postorbitals and a long interpterygoid vacuity, includes *Tropidostoma* and *Oudenodon*, but not *Rhachiocephalus* (Angielczyk 2001). Of these taxa, teeth are present in *Tropidostoma* but lacking in *Oudenodon*.
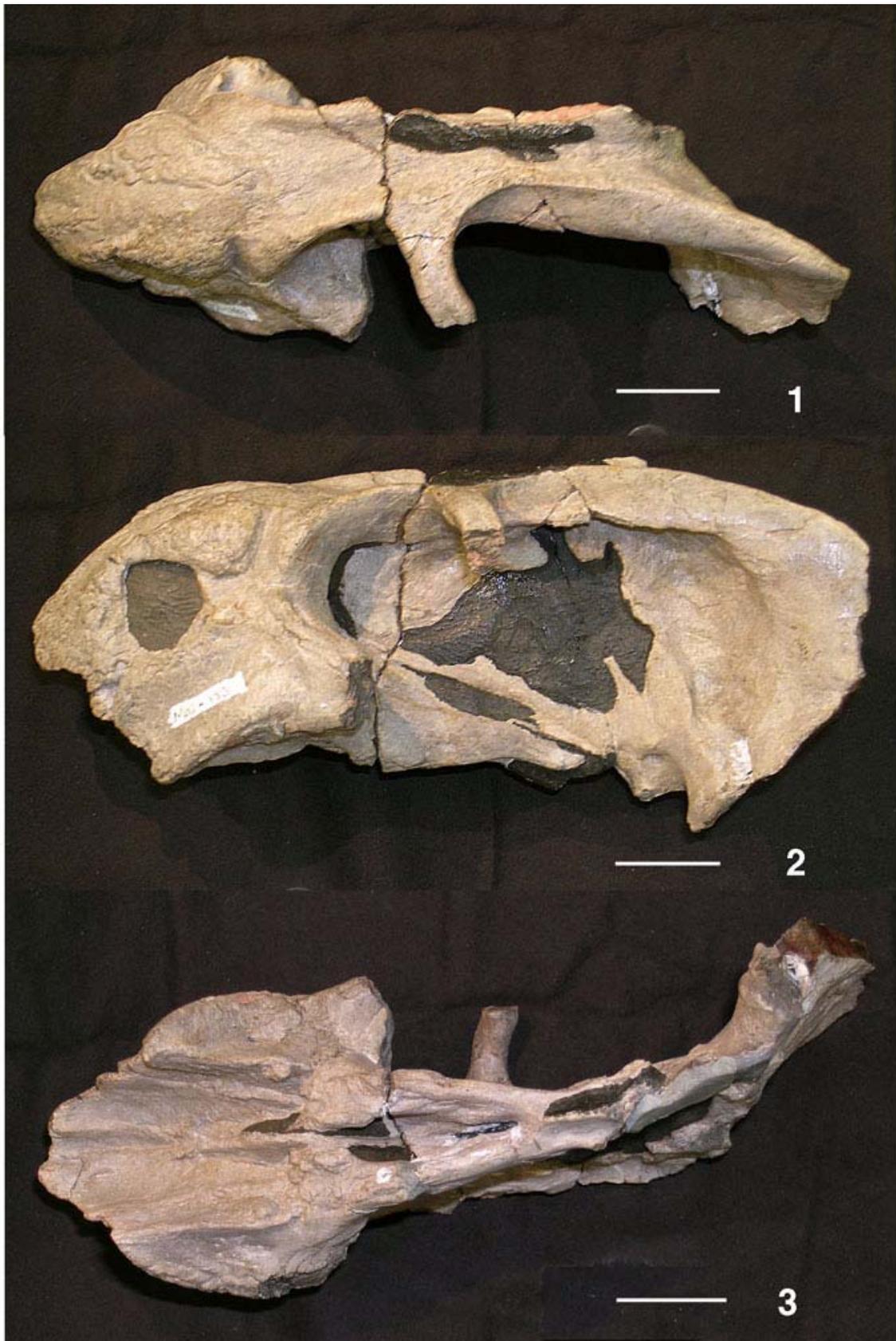
Figure 6. *Oudenodon* sp. (Mal 108) from the Chiweta Beds, Malawi, (1.1) dorsal view, (1.2) left lateral view, (1.3) palatal view. Scale bars are 30 millimeters.

Figure 7. *Oudenodon* sp. (Mal 129) from the Chiweta Beds, Malawi, (1.1) dorsal view, (1.2) palatal view. Scale bars are 30 millimeters.

Table 2. Measurements (mm) of *Oudenodon* skulls from the Chiweta Beds, Malawi.

	Mal 108	Mal 129
Basal skull length	216	208
Preorbital length	83	84
Longitudinal orbital diameter	50	40
Postorbital bar width	11	11
Interorbital width	30	33
Intertemporal width	29	38
Longitudinal pineal diameter	715	7
Length to pineal foramen	149	139
Palatal length	84	84
Width between caniniform processes	40	50

Haughton (1926) reported two species of *Dicynodon* distinguished by size in the material sent him by Dixey from Chiweta. Both are tuskless. The illustrations in Haughton (1926) of the smaller species, designated by him *Dicynodon* sp. A, show the parietals exposed between the postorbitals, indicating that it should be referred to *Oudenodon*. The larger species was represented by a fragmentary skull, a humerus, and parts of other postcranial bones, which Haughton designated *Dicynodon* sp. cf. *D. grandis*. The referral of those specimens to *D. grandis*, a species named by Haughton (1917), was based on size alone. Keyser (1975), in his review of tuskless anomodonts, referred *D. grandis* to the genus *Oudenodon*, consolidating the genus and synonymizing a large number of species into three: *O. baini*, the genotype, most abundant, and widespread species; *O. grandis*, a rare but large species whose only diagnostic character other than size is having the parietal foramen lie in a depression on the dorsal surface of the skull; and *O. luangwaensis*, known from Zambia and defined on the basis of "…the great width of the zygomatic arches, giving the skulls their very characteristic heart shape" (Keyser 1975, p. 57).

Measurements of Mal 108 and Mal 129 (Table 2) fall within the range of *Oudenodon baini* presented by Keyser (1975, p. 39-40) indicating that those specimens do not pertain to *O. grandis*. In addition, a low boss lies near the parietal foramen of Mal 108, which if a reliable character, also indicates that Mal 108 is not *O. grandis*. Mal 129 lacks the great width and therefore the "very characteristic heart shape" of the skull of *O. luangwaensis*, even though this character in Mal 129 is accentuated by dorsoventral flattening. Haughton's *Dicynodon* sp. A is smaller than either Mal 108 or Mal 129, but still within the range of *O. baini*. We therefore identify Mal 108, 129, and *Dicynodon* sp. A of Haughton (1926) as *Oudenodon baini*.

Haughton (1926) also reported teeth and jaw fragments of *Endothiodon* cf. *E. bathystoma*. He questioned the level from which they were obtained but considered them most likely to come from the Lower Bone Bed (B1), and therefore less likely to have come from the Upper Bone Bed (B2). We have not recorded *Endothiodon* in the collections we made from B1. Regardless, *Endothiodon* is a distinctive genus (Cox 1964) and its occurrence in the Chiweta Beds has biostratigraphic significance. Haughton (1926, p. 82), in evaluating the age of the Chiweta fauna, states, "…had [the assemblage] been found in South Africa, [it] would unhesitatingly have been assigned to the base of the *Cistecephalus* zone or top of the *Endothiodon* zone of the Lower Beaufort Beds."

Numerous revisions to the biostratigraphy of the Beaufort Group have been made since Haughton's work, but his observations are on the mark. In the latest comprehensive revision, *Endothiodon* is a component of the upper *Pristerognathus* Assemblage Zone (Smith and Keyser 1995a), the *Tropidostoma* Assemblage Zone (Smith and Keyser 1995b), and at least the lower portion of the *Cistecephalus* Assemblage Zone (Smith and Keyser, 1995c). *Oudenodon* is found throughout the *Cistecephalus* and the overlying *Dicynodon* assemblage zones (Kitching 1995), becoming extinct near the Permian-Triassic boundary. *Gorgonops* is known from the *Tropidostoma* and most of the *Cistecephalus* Assemblage Zones (Smith and Keyser 1995b). Thus, the overlapping ranges of *Endothiodon* and *Oudenodon*, consistent with the presence of *Gorgonops*? *dixeyi* and *Aelurognathus*, argue for a lower *Cistecephalus* Assemblage Zone placement for the Chiweta Beds. The youngest likely age falls just below the midpoint of the Tatarian Stage (Hancox and Rubidge 2001), or following Gradstein and Ogg (2004), about at the middle of the Wuchiapingian Stage, or approximately 256 to 258 Ma. We take that range as a best estimate for the age of the fauna.

In conjunction with his phylogenetic analyses of dicynodonts, Angielczyk (2001, 2002; Angielczk and Kurkin 2003a, 2003b) fitted preferred cladograms to the stratigraphic record of the taxa, thereby demonstrating the extent of ghost lineages associated with most parsimonious trees. The most significant implication for this study affects the overlap between *Endothiodon* and *Oudenodon*, a co-occurrence that limits the correlation of the Chiweta Beds with the *Cistecephalus* Assemblage Zone, but eliminates a correlation with the uppermost portion of that same zone. The downward ghost extension of *Oudenodon*, it might be argued, could affect the correlation of the Chiweta Beds

with the Karoo Basin of South Africa by allowing a correlation with the underlying *Tropidostoma* Assemblage Zone. However, the biostratigraphic ranges of the robust suite of pollen taxa (Yemane 1994) limit the maximum age of the therapsid assemblage and mitigate concern over downward extension of the *Oudenodon* range.

SYSTEMATIC PALEONTOLOGY

THERAPSIDA Broom, 1905
BIARMOSUCHIA Sigogneau-Russell, 1989
BURNETIAMORPHA Broom, 1923

Definition. The most inclusive clade including *Burnetia mirabilis*, but excluding *Biarmosuchus tener*, *Hipposaurus boonstrai*, and *Ictidorhinus martinsi* (from Sidor and Wellman 2003, p. 631).

Diagnosis. Supraorbital boss present, antorbital fossa or pit on lateral surface of lacrimal; median frontal ridge present but variably expressed; boss on ventral surface of squamosal lateral to level of quadrate; boss present on lower margin of zygomatic arch at level of postorbital bar (from Sidor and Welman 2003, p. 632).

Unnamed New Genus and Species

Material. A nearly complete skull, slightly distorted and damaged in the premaxillary region.

Diagnosis. Mal 290 has a skull roof that is relatively unpachyostotic; posteriorly directed squamosal boss at dorsal apex of lateral temporal fenestra present, but not developed into squamosal horns; narrow median nasal boss present. Its autapomorphies include: short facial region, large orbit, and frontal and supraorbital bosses of equal height. For other characters see phylogenetic analysis.

Occurrence. Lower Bone Bed (B1) of the Chiweta Beds, Malawi.

Comments. Mal 290 exhibits all of the features of Burnetiamorpha listed above, although the zygomatic boss is either poorly preserved or poorly developed. The description and phylogenetic analysis demonstrates that Mal 290 is a new taxon, but we are working from a cast in this study. As stated in the Introduction, Elizabeth M. Gomani will oversee final description, analysis, and naming of this taxon in conjunction with a more detailed study of the Chiweta Beds and its fauna.

Description of Mal 290

Mal 290 (Table 3, Figures 8, 9) is nearly complete but slightly distorted and with the lower jaw attached. The right side has been pushed posteriorly with the anterior portion rotated ventromedially.

Table 3. Measurements (mm) of a new burnetiid biarmosuchian therapsid from the Chiweta Beds, Malawi.

	Mal 290
Basal skull length	150
Preorbital length	48
Longitudinal orbital diameter	36.8
Postorbital bar width	11.5
Interorbital width	33.8
Intertemporal width	58.7
Longitudinal pineal diameter	5
Length to pineal foramen	101
Length to pterygoid transverse flange	67.7

The anterior premaxillary and nasal region is damaged so incisor relationships are not obvious. The lower jaw is attached with the left ramus in articulation. The right ramus is damaged and pushed posteriorly with its posterior portion rotated medially more than the anterior portion. Sutures are obscure, usually an indication that a specimen is not juvenile, but burnetiamorph sutures tend to be difficult to discern and their obscurity may not rule out Mal 290 being juvenile. Other features that might reflect a juvenile state are the large size of the lateral temporal fenestra, large orbits, and short facial region (Sidor personal commun., 2004).

The broadest transverse dimension of the skull is across the squamosals at the level of the zygomatic arch at the ventral margin of the lateral temporal fenestra. The posterior outline viewed from above is gently concave. The skull is narrow across the frontals and tapers anteriorly. In lateral view, the skull is deep, highest at the supraorbital bosses, but the lower jaw is shallow and not expanded anteriorly to any great degree. The orbit is round and larger than the lateral temporal fenestra, which is also nearly round and situated in the posteroventral area of the skull. The narrow snout is short (length approximately 120% of diameter of the orbit), but longer than the postorbital length (approximately equal to orbital diameter). The occipital region is vertical (perpendicular to the tooth row). The frontals contain the highest point on the skull, from which the parietal region angles steeply to the dorsal margin of the occipital region. The pineal foramen lies in a diffuse crater-like swelling nearly in line with the posterior margin of the orbit and slightly anterior to the plane of the occipital condyle. Anteriorly the skull slopes less steeply toward the snout.

There is minor anteroposterior shearing deformation of the supraorbital bosses relative to the frontal boss and minor dorsal extension of the left supraorbital boss relative to the right. Assuming all
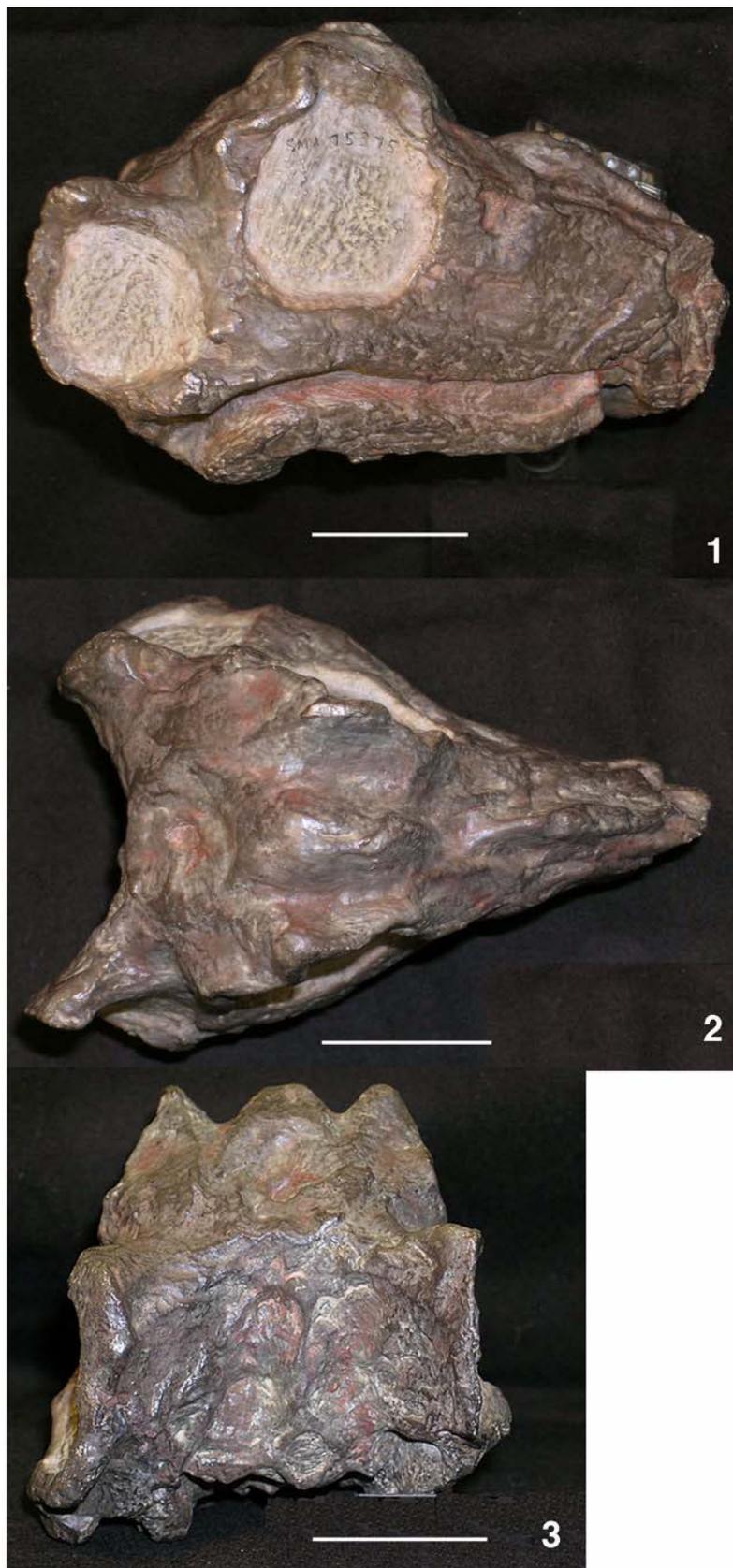
Figure 8. Unnamed burnetiid (Mal 290) from the Chiweta Beds, Malawi, (1.1) right lateral view, (1.2) dorsal view, (1.3) posterior view. Scale bars are 30 millimeters.
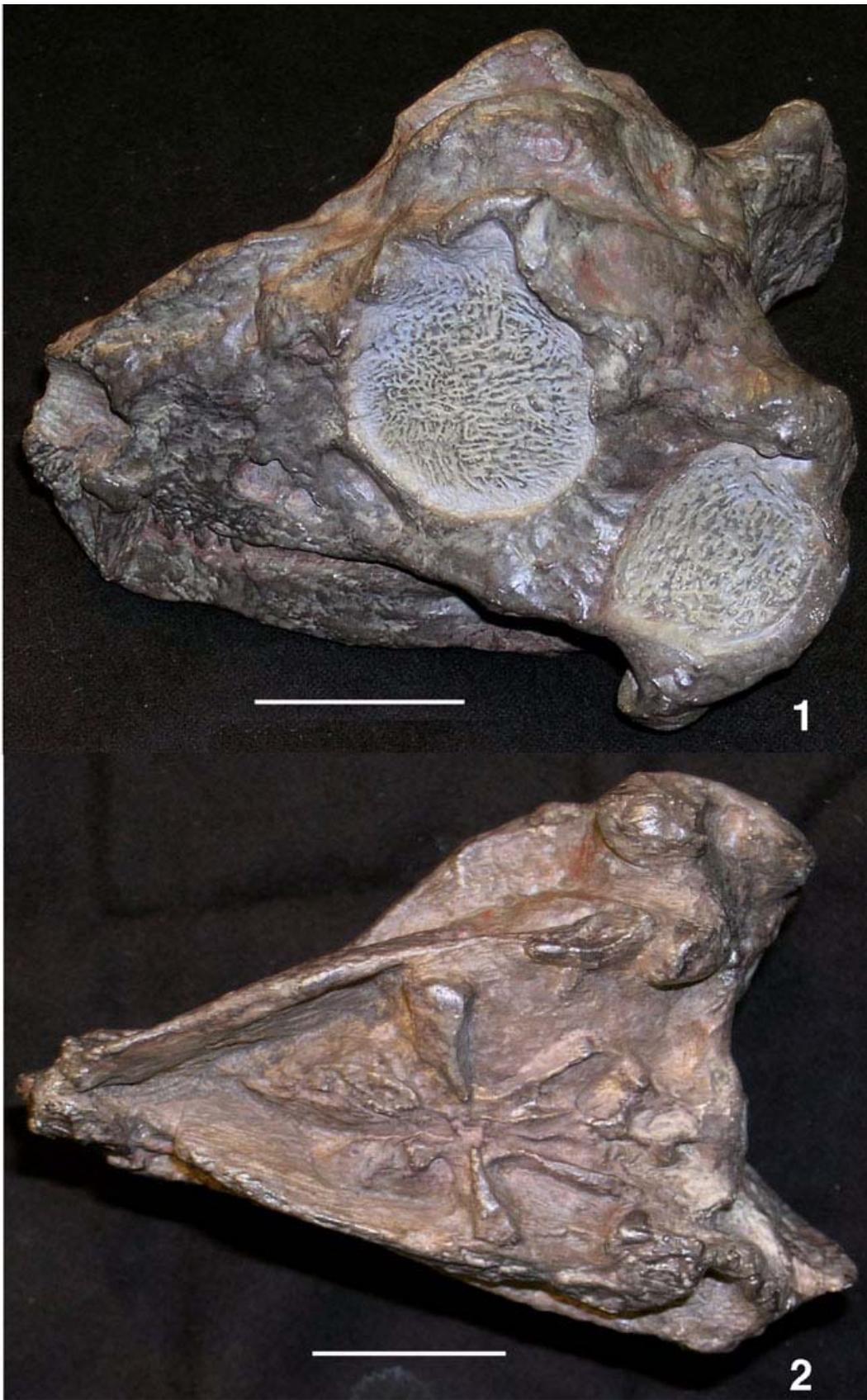
Figure 9. Unnamed burnetiid (Mal 290) from the Chiweta Beds, Malawi, (1.1) left oblique view, (1.2) palatal view. Scale bars are 30 millimeters.

deformation is recognized, the supraorbital bosses are well developed and of comparable height to the broad median frontal boss. The frontal boss is widely separated from a distinct, narrow, median nasal boss, which extends toward the snout from the plane of the anterior margin of the orbit. It is highest posteriorly, tapering gradually to the nose, terminating at the posterior margin of the external nares. A boss occurs at the posterodorsal margin of the orbit near the origin of the postorbital bar. A well-developed boss is found on the squamosal at the dorsal margin of the lateral temporal fenestra but it is not developed into a squamosal horn. A poorly preserved or weakly developed boss occurs on the zygomatic arch at the level of the postorbital bar. The zygomatic arch is bent strongly ventrally.

The dorsal process of the premaxilla is short and does not extend to a level posterior to the canine as indicated by the narrowness of the snout. The septomaxilla is exposed on the face. Fossae are present in the position of the lacrimal, although sutures are difficult to discern. The posterior extent of the postorbital onto the margin of the lateral temporal fenestra is unclear, but it does not appear to extend to the posterior margin of the lateral temporal fenestra because of the squamosal boss developed along the posterodorsal margin. The medial portion of the squamosal overlaps the quadrate.

The anterior portion of the palate has not been prepared so the vomer and the vomerine process of the premaxillae cannot be seen, nor can the anterior portion of the palatines. The ectoptygoids are not visible. The transverse flanges of the pterygoids lie beneath the anterior half of the orbit and appear to have denticles. The basicranial rami of the pterygoids exhibit a median trough defined by parasagittal ridges. The parabasisphenoid has a ventral fossa and apparently lacks a midline ridge. It extends back to the basioccipital at the occipital condyle.

The occipital condyle is small. The relationship of the exoccipitals on the dorsal side of the foramen magnum is unclear. A ridge extends dorsally from the foramen magnum to the dorsal margin of the postparietal. Given the width of the posterior portion of the skull between the tabulars, the postparietal appears to be approximately square. A posttemporal fenestra lies dorsal to the paroccipital process. The stapes is not visible.

The mandibular symphysis is unfused. The level of the base of the dentary follows a sinuous curve, but the bone is relatively shallow. The shape of the dentary-angular suture is unclear. Ridges and fossae occur on the angular. The articular is unprepared. There is no fenestra between angular

and dentary. The surangular has a laterally projecting ridge. The jaw articulation lies below the level of the tooth row. The medial surface of the jaw is unprepared.

The upper incisors are not preserved, but they could not have been as large as the canine. At least six postcanine teeth are visible on the left side of the skull, although serrations cannot be discerned. The area around the left upper canine is slightly crushed, but the remnants of the right canine suggest a slight anterior orientation and a short diastema between the canine and postcanine dentition. The lower canine is unprepared, and no dentary teeth can be seen.

Phylogenetic Position of Mal 290

Phylogenetic analysis was performed using PAUP 4.0 Beta 10 and MacClade 4.06 on the data matrix of 37 characters presented by Sidor and Welman (2003), with character 30 (of Sidor and Welman 2003; ratio of dentary height in canine versus anterior postcanine regions) deleted because we found the scoring confusing, and with Mal 290 added to bring the total number of taxa to 13 (Appendix, Table 4). We chose this data set because it includes taxa in which we are most interested, notably *Lemurosaurus* and the burnetiids *Proburnetia*, *Burnetia*, and *Bullacephalus*. This group, the Burnetiamorpha, falls within the Biarmosuchia, originally considered to be defined on primitive characters but now accepted as monophyletic (Hopson 1991; Hopson and Barghusen 1986; Rubidge and Kitching 2003; Rubidge and Sidor 2001, 2002; Sidor 2001, 2003; Sidor and Hopson 1998; Sidor and Welman 2003; Sigogneau-Russell 1989). The sphenacodontid synapsids *Haptodus* and *Dimetrodon* were specified as outgroups, as in Sidor and Welman (2003). In most cases, the operational taxonomic units in the data matrix are genera, except for the family level group Anteosauridae and the single, taxonomically undesignated specimen Mal 290. Multistate characters were treated as unordered. All characters were equally weighted. Unknown or inapplicable characters were scored with a question mark. Branch and bound searches found three most parsimonious trees with lengths of 55, consistency indices of 0.82, and retention indices of 0.86.

All three most parsimonious cladograms and the strict consensus tree (Figure 10) exhibit identical topologies among *Ictidorhinus*, *Lemurosaurus*, Mal 290, *Proburnetia*, *Bullacephalus*, and *Burnetia*. Mal 290 forms a monophyletic clade with the Burnetiidae, which includes *Burnetia*, *Proburnetia*, and *Bullacephalus*. Mal 290 is united with the Burnetiidae by two unambiguous characters, (Appendix 1,

14
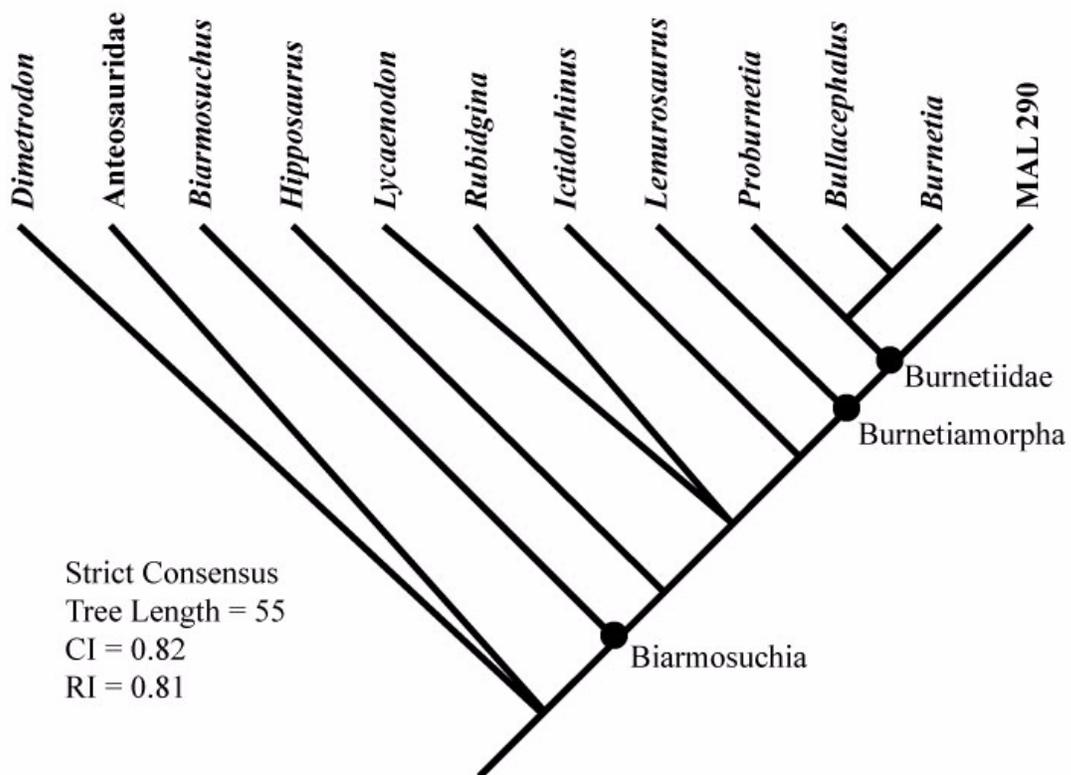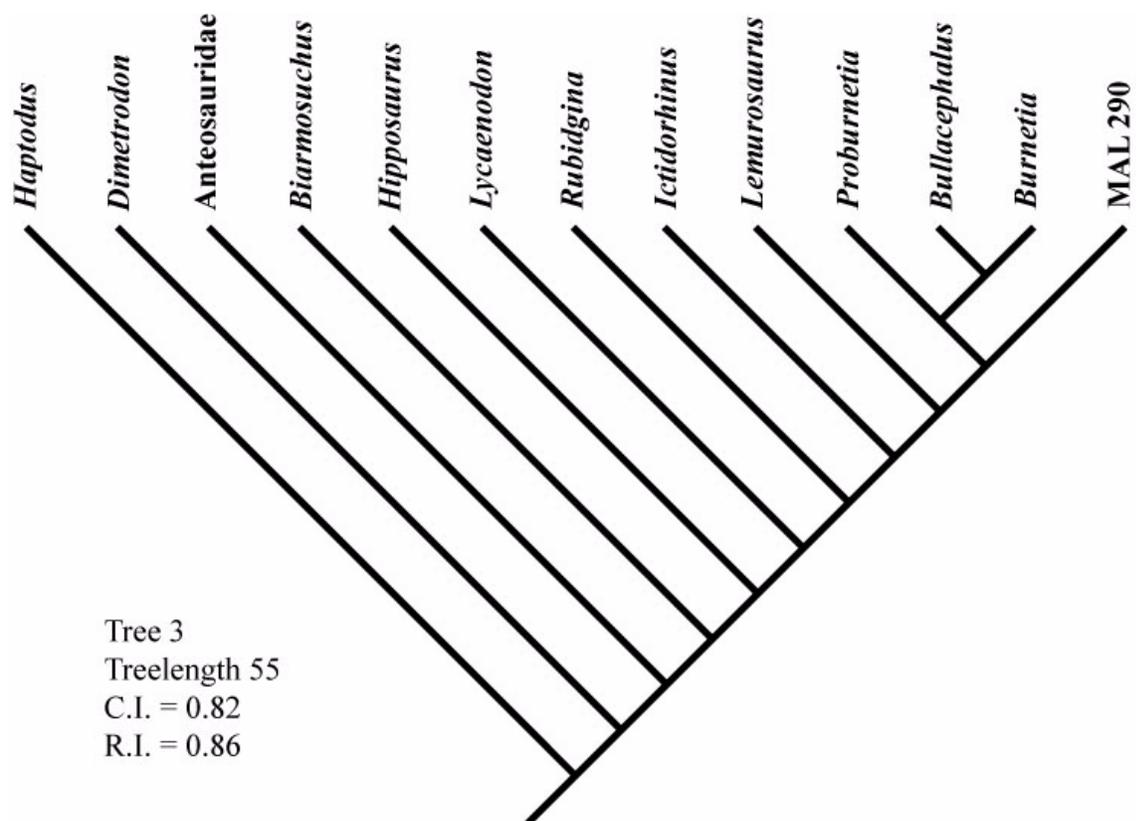
Figure 10. One of the three most parsimonious trees (top) and the strict consensus tree (bottom) showing the placement of Mal 290 more derived than *Lemuosaurus* and sister to other Burnetiidae (*Proburnetia*, *Burnetia*, and *Bullacephalus*).

Table 4. Data matrix modified from Sidor and Welman (2003) used in the cladistic analysis of Mal 290.

Haptodus	0	0	0	0	0	0	0	0	0	0	0	0	0	0	0	0	0	0	0	0
Dimetrodon	0	0	0	0	0	0	0	0	0	0	0	0	0	0	0	0	0	0	0	0
Anteosauridae	0	1	1	0	1	0	0	0	0	0	0	0	0	0	0	2	0	1	0	0
Biarmosuchus	?	1	1	0	1	0	0	0	0	0	0	0	0	0	0	2	0	1	?	0
Hipposaurus	?	1	1	0	1	0	0	0	?	?	?	0	0	0	1	2	1	1	?	1
Lycaenodon	1	0	1	0	1	0	0	0	?	?	?	?	?	0	?	2	1	?	1	1
Rubidgina	?	0	1	0	1	0	0	0	0	0	0	0	0	0	1	2	1	1	1	1
Ictidorhinus	1	?	1	?	1	?	1	0	0	?	0	0	?	1	?	2	?	?	?	?
Lemurosaurus	?	?	1	1	1	0	2	0	1	0	1	0	0	1	1	2	?	?	1	1
Proburnetia	1	0	1	1	?	1	2	0	1	1	1	1	1	2	0	1	?	?	1	1
Bullacephalus	?	?	?	1	1	2	2	1	?	1	1	?	1	0	?	1	?	?	1	1
Burnetia	1	?	1	1	?	2	2	1	1	1	1	1	1	1	?	1	?	?	?	1
Mal 290	?	0	1	1	1	1	2	1	1	0	1	0	0	2	?	1	?	?	?	1

character 6) nasal eminence (although the nasal eminence in *Proburnetia* is not like *Burnetia* nor *Bullacephalus*) and (character 16) circum-pineal parietal shape (which might be considered distinct in *Bullacephalus*), in two most parsimonious trees. The burnetiids, exclusive of Mal. 290, are defined by (character 10) thickening of the squamosal lateral to quadrate, (character 12) squamosal horns present, and (character 13) squamosal thickened along its posterior border with tabular. Within the Burnetiidae, *Burnetia* and *Bullacephalus* consistently fall as a derived sister group to *Proburnetia*, as was concluded by Sidor and Welman (2003), because the nasal boss is scored as transversely expanded (character 6).

The definition of Burnetiamorpha cited by Sidor and Welman (2003, p. 631) is, "The most inclusive clade including *Burnetia mirabilis*, but excluding *Biarmosuchus tener*, *Hipposaurus boonstrai*, and *Ictidorhinus martinsi*." *Ictidorhinus*, shown as the next taxon out from Burnetiamopha, is a poorly known taxon with 57% of its characters scored as question mark. It is weakly linked to Burnetiamorpha. The more basal portion of the tree follows Sidor and Welman (2003) and needs not be discussed here.

DISCUSSION AND CONCLUSIONS

The Karoo LIP (Marsh et al. 1997, 2004) is bounded by the Drakensberg Volcanics on the south, the Lebombo Mountains of Swaziland and Mozambique to the east, the Etjo Formation of northeast Namibia on the west, and the Batoka, Lupata, and Chikwawa basalts of Zimbabwe, Mozambique, and Malawi to the north. Fitch and Miller (1984) reviewed radiometric dates from southern Africa and concluded that lavas were progressively younger from south to north, and that the distribution of dates showed episodic centers of volcanic activity. A range of dates from Middle Jurassic to Cretaceous was indicated. There are indeed Cretaceous volcanic rocks in Malawi, particularly ring structures and carbonatites (Dixey et al. 1955; Garson 1965). However, Duncan et al. (1997); Marsh et al. (1997); and Jones et al. (2001) demonstrate with new data that Karoo LIP basalts were erupted in a narrow range of time, as were similar basalts in Antarctica, at 184-179 Ma. This narrow clustering of dates characterizes the flood basalt eruptions associated with the rifting of eastern Gondwana. As such, the Karoo LIP is a component of the larger Karoo-Farrar Magmatic Province, which represents one of the largest known continental flood basalt events, extending from Africa, across Antarctica, and into Tasmania and Australia (Duncan et al. 1997). At its western geographic extreme, Karoo LIP basalt extends to 18° E in Namibia, in close proximity to the Early Cretaceous African and South American Parana-Etendeka Flood Basalt Province. That Cretaceous volcanic province is associated with rifting of western Gondwana and the opening of the South Atlantic.

In addition to heralding the tectonic reshaping of continental landmasses, flood basalt events coincide with some extinction events. The vast flood basalt eruptions of the Karoo-Farrar Magmatic Province have been implicated in the moderate Toarcian-Aalenian extinctions affecting marine invertebrates (Duncan et al. 1997). Nevertheless, even accepting an affect on marine invertebrates, the effects of the volcanic event that produced the Karoo-Farrar Magmatic Province on therapsids is unclear.

Of the fossils from the Chiweta Beds, our focus on dicynodonts was to refine the age of the Chiweta Beds; in studying Mal 290 it has been to evaluate its position among the taxa included by Sidor and Welman (2003) in their analysis of the burnetiamorph *Lemurosaurus*. In the interim, Sidor et al. (2004) described a new basal burnetiamorph

Table 4 (continued).

Haptodus	0	0	0	0	0	0	0	?	?	0	0	0	0	0	0	?	0
Dimetrodon	0	0	0	0	0	0	0	0	0	0	0	0	0	0	0	1	0
Anteosauridae	?	1	1	2	2	1	?	0	2	0/1	0	0	0	0	2	1	1
Biarmosuchus	0	1	0	1	1	1	1	?	1	1	1	1	1	1	1	?	1
Hipposaurus	0	1	0	1	1	1	1	?	1	1	1	1	1	1	1	?	1
Lycaenodon	1	1	1	1	1	?	?	?	?	?	?	?	?	1	?	0	1
Rubidgina	1	1	1	1	1	1	?	1	1	1	1	1	1	1	1	?	1
Ictidorhinus	?	1	1	?	?	?	?	?	1	?	?	?	?	1	?	0	?
Lemurosaurus	1	1	1	1	1	1	1	?	1	1	1	?	1	1	1	?	1
Proburnetia	?	1	1	1	1	1	1	1	1	1	1	?	?	1	1	0	1
Bullacephalus	0	1	0	2	1	1	?	?	1	1	1	1	1	?	?	?	1
Burnetia	?	1	1	1	1	1	?	?	0	?	?	?	?	?	?	0	1
Mal 290	1	?	1	1	1	1	?	?	1	?	1	?	1	1	?	?	1

with a systematic analysis including the Russian taxon *Niuksenitia* (see also Battail and Surkov 2000) and an unnamed South African taxon. Including Mal 290, this brings to half a dozen the number of taxa (named or unnamed) that can be included in the Burnetiidae, with two more added in the more inclusive Burnetiamorpha. None of the taxa is well known and their stratigraphic distribution suggests numerous long ghost lineages. However, another possibility is that as characters are discerned and refined, phylogenetic analyses may yield trees with different topologies.

The nasal boss of *Bullacephalus* is more circular in cross section than that of *Burnetia*, which has likewise been scored as having a transversely expanded nasal boss. The presence of squamosal horns in *Bullacephalus* is also in question. In addition, the position of the pineal foramen on the dorsal surface of the skull reflects the orientation of the parietals, which are less inclined than in *Burnetia* and Mal 290, assuming no significant taphonomic distortion. The skull bones of *Bullacephalus* are clearly pachyostotic, and the genus is derived in that feature, but given its other features, and as new burnetiamorphs come to light, a re-evaluation of its status may become warranted.

The therapsids of the Chiweta Beds are interesting paleogeographically when considered in the context of the northern Malawi Karoo. Smith et al. (1993) interpreted the climate during the deposition of the Beaufort Group in South Africa as semi-arid with highly seasonal rainfall. In Malawi, Yemane et al. (1989) hypothesized a string of large, interconnected lakes of such a geographic extent that they ameliorated the rigors of climate at paleolaltitudes between 45° and 60° S (Yemane 1993). Based on oxygen isotopic studies of carbonate concretions found within the lacustrine sediments underlying the Chiweta Beds, Yemane and Kelts (1996), suggested mean annual surface temperatures possibly as high as 10°C, comparable to those of continental temperate climates, such as that of Switzerland today.

There is no evidence as to what the therapsid fauna was like at the time the region was covered by large lacustrine systems, but by the time of deposition of the Chiweta Beds, the lakes were gone from that area of Malawi, as far as can be determined from the rocks that remain. The Chiweta therapsids seem to have existed in a fluvially dominated ecosystem similar to that existing to the south. Their range of tolerances is unknown, but the presence of *Oudenodon* in the lower *Cistecephalous* Assemblage Zone of Malawi may indicate rather wide tolerances and an ability to maintain its niche as suitable habitat became available. On the other hand, Mal 290, as representative of a new burnetiid taxon, might indicate that the invasion of new territory following environmental change was an important factor in the diversification of burnetiamorphs.

data, we thank K.D. Angielczyk, J. Hancox, G. King, N. Macleod, M.J. Polcyn, B. Rubidge, C. Sidor, and R. Smith. We learned a great deal from all of these colleagues. This paper has benefited from thorough reviews by K.D. Angielczyk, B. Rubidge, and C. Sidor, although we do not necessarily expect them to heartily accept all of our accommodations to their comments, and they are certainly not responsible for any decisions we may have taken. We acknowledge our deep appreciation of the late N. Hotton, III, who enabled the preparation of Mal 129, showed us specimens, and discussed Karoo vertebrates with us. With this contribution our proud association in the African field with W. Downs is brought to a close.

REFERENCES

Andrew, A.R. and Bailey, T.E.G. 1910. The geology of Nyasaland. *Quarterly Journal of the Geological Society of London*, 66:189-237.

Angielczyk, K.D. 2001. Preliminary phylogenetic analysis and stratigraphic congruence of the dicynodont anomodonts (Synapsida: Therapsida). *Palaeontologia Africana*, 37:53-79.

Angielczyk, K.D. 2002. A character-based method for measuring the fit of a cladogram to the fossil record. *Systematic Biology*, 51(1):176-191.

Angielczyk, K.D., and Kurkin, A.A. 2003a. Has the utility of *Dicynodon* for late Permian terrestrial biostratigraphy been overstated? *Geology*, 31(4):363-366.

Angielczyk, K.D., and Kurkin, A.A. 2003b. Phylogenetic analysis of Russian Permian dicynodonts (Therapsida: Anomodontia): implications for Permian biostratigraphy and Pangaean biogeography. *Zoological Journal of the Linnean Society*, 139:157-212.

Arber, E.A.N. 1910. Note on a collection of fossil plants from the neighborhood of Lake Nyasa, collected by Mr. A.R. Andrew. *Quarterly Journal of the Geological Society of London*, 66:237-239.

Bangert, B., Stollhofen, H., Lorenz, V., and Armstrong, R. 1999. The geochronology and significance of ash-fall tuffs in the glaciogenic Carboniferous-Permian Dwyka Group of Namibia and South Africa. *Journal of African Earth Sciences*, 29:33-49.

Battail, B. and Surkov, M.V. 2000. Mammal-like reptiles from Russia, p. 86-119. In Benton, M.J., Shishkin, M.A., Unwin, D.M., and Kurochkin, E.N. (eds.), *The Age of Dinosaurs in Russia and Mongolia*. Cambridge University Press, Cambridge, UK.

Best, M.G., Christiansen Best, M.G., Christiansen, E.H., Deino, A.L., Grommé, C.S., and Tingey, D.G. 1995. Correlation and emplacement of a large, zoned, discontinuously exposed ash-flow sheet: ^{40}Ar/^{39}Ar chronology, paleomagnetism, and petrology of the Pahranagat Formation, Nevada. *Journal of Geophysical Research,* 100: B12:24593-24609.

Bordy, E.M., Hancox, P.J., and Rubidge, B.S. 2004. Fluvial style variations in the late Triassic-early Jurassic Elliot Formation, main Karoo Basin, South Africa. *Journal of African Earth Sciences*, 38:383-400.

Broom, R. 1905. On the use of the term Anomodontia. *Records of the Albany Museum*, 1:266-269.

Broom, R. 1923. On the structure of the skull in the carnivorous dinocephalian reptiles. *Proceedings of the Zoological Society of London*, 2:661-684.

Cairncross, B. 2001. An overview of the Permian (Karoo) coal deposits of southern Africa. *Journal of African Earth Sciences*, 33:529-562.

Cooper, W.G.G. and Habgood, F. 1959. The geology of the Livingstonia Coalfield. *Nyasaland Geological Survey Bulletin*, 11:1-51.

Cox, C.B. 1964. On the palate, dentition, and classification of the fossil reptile *Endothiodon*. *American Museum Novitates*, 2171:1-25.

Cox, K.G. 1970. Tectonics and vulcanism orf the Karroo Period and their bearing on the postulated fragmentation of Gondwanaland, p. 211-235. In Clifford, T.N. and Gass, I.G. (eds.), *African magmatism and tectonics*. Oliver and Boyd, Ltd., Edinburgh.

Deino, A., Tauxe, L., Monaghan, M., and Drake, R. 1990. Single-crystal $_{40}$Ar/^{39}Ar ages and the litho- and paleomagnetic stratigraphies of the Ngorora Formation, Kenya. *Journal of Geology*, 98:567-587.

Dixey, F. 1926. Notes on the Karroo sequence northwest of Lake Nyasa. *Transactions of the Geological Society of South Africa*, 29:59-68.

Dixey, F. 1928. The Dinosaur Beds of Lake Nyasa. *Transactions of the Royal Society of South Africa*, 16:55-66.

Dixey, F. 1930. The Karroo of the lower Shire-Zambezi area. *International Geological Congress*, 15:120-132.

Dixey, F. and Smith, W.C. 1929. The rocks of the Lupata Gorge and the north side of the lower Zambezi. *Geological Magazine*, 66:241-259.

Dixey, F., Smith, W.C., and Bisset, C.B. 1955. The Chilwa Series of southern Nyasaland. *Nyasaland Protectorate Geological Survey Department Bulletin*, 5:1-71.

Drummond, H. 1884. Geology of Central Africa. *Nature*, 29:551.

Drummond, H. 1888. *Tropical Africa*. Hodder and Stoughton, London.

Du Toit, A.L. 1926. *The Geology of South Africa*. Oliver and Boyd, Ltd., Edinburgh.

Duncan, R.A., Hooper, P.R., Rehacek, J., Marsh, J.S., and Duncan, A.R. 1997. The timing and duration of the Karoo igneous event, southern Gondwana. *Journal of Geophysical Research*, 102: B8:18,127-18,138.

Fitch, F.J. and Miller, J.A. 1984. Dating Karoo igneous rocks by the conventional K-Ar and ^{40}Ar/^{39}Ar age spectrum methods. *Geological Society of South Africa, Special Publication*, 13:247-66.

Gay, S.A. and Cruickshank, A.R.I. 1999. Biostratigraphy of the Permian tetrapod faunas from the Ruhuhu Valley, Tanzania. *Journal of African Earth Sciences*, 29:195-210.

Garson, M.S. 1965. Carbonatites in southern Malawi. *Malawi Geological Survey Department Bulletin*, 15:1-128.

Gradstein, F.M. and Ogg, J.G. 2004. Geologic time scale 2004 – why, how, and where next! *Lethaia*, 37:175-181.

Habgood, F. 1963. The geology of the country west of the Shire River between Chikwawa and Chiromo. *Malawi Geological Survey Bulletin*, 14:1-60.

Hancox, P.J., Brandt, D., Reimold, W.U., Koeberl, C., and Neveling, J. 2002. Permian-Triassic boundary in the northwest Karoo basin: Current stratigraphic placement, implications for basin development models, and the search for evidence of impact. *Geological Society of America, Special Paper*, 356:429-444.

Hancox, P.J. and Rubidge, B.S. 2001. Breakthroughs in the biodiversity, biogeography, biostratigraphy, and basin analysis of the Beaufort group. *Journal African of Earth Sciences*, 33:563-577.

Haughton, S.H. 1917. Descriptive catalog of the Anomodontia with especial reference to the examples in the South African Museum. *Annals of the South African Museum*, 12:127-174.

Haughton, S.H. 1926. On Karroo vertebrates from Nyasaland. *Transactions of the Geological Society of South Africa*, 29:69-83.

Haughton, S.H. 1928. On some reptilian remains from the Dinosaur Beds of Nyasaland. *Transactions of the Royal Society of South Africa*, 16:67-75.

Hopson, J.A. 1991. Systematics of the non-mammalian Synapsida and implications for patterns of evolution in synapsids, p. 635-693. In Schultze, H.-P. and Trueb, L. (eds.), *Origins of the Higher Groups of Tetrapods*. Comstock Publishing Associates, Ithaca, New York.

Hopson, J.A. and Barghusen, H.R. 1986. An analysis of therapsid relationships, p. 83-106. In Hotton, N., III, MacLean, P.D., Roth, J.J., and Roth, E.C. (eds.), *The Ecology and Biology of Mammal-like Reptiles*. Smithsonian Institution Press, Washington, D.C.

Jacobs, L.L. 1993. *Quest for the African Dinosaurs*. Villard Books, New York.

Jacobs, L.L., Winkler, D.A., and Downs, W.R. 1992. Malawi's paleontological heritage. *Occasional Papers of the Malawi Department of Antiquities*, 1:5-22.

Jacobs, L.L., Winkler, D.A., Downs, W.R., and Gomani, E.M. 1993. New material of an Early Cretaceous titanosaurid sauropod dinosaur from Malawi. *Palaeontology*, 36:523-534.

Johnson, M.R., Van Vuuren, C.J., Hegenberger, W.F., Key, R., and Shoko, U. 1996. Stratigraphy of the Karoo Supergroup in southern Africa: An overview. *Journal of African Earth Sciences*, 23:3-15.

Jones, D.L., Duncan, R.A., Briden, J.C., Randall, D.E., and MacNiocaill, C. 2001. Age of the Batoka basalts, northern Zimbabwe, and the duration of Karoo Large Igneous Province magmatism. *Geochemistry, Geophysics, Geosystems*, 2, 2000GC000110.

Jones, T. R. 1890. On some fossils from Central Africa. *Geological Magazine*, 7:409-410.

Keyser, A.W. 1975. A re-evaluation of the cranial morphology and systematics of some tuskless Anomodontia. *Memoirs of the South Africa Geological Survey*, 67:1-110.

King, G.M. 1988. *Anomodontia. Encyclopedia of Paleoherpetology*. Gustav Fischer Verlag, Stuttgart.

King, G.M. 1990. *The Dicynodonts: A Study in Paleobiology*. Chapman and Hall, London.

Kitching, J.W. 1995. Biostratigraphy of the *Dicynodon* Assemblage Zone. *Geological Survey of South Africa, South African Committee for Stratigraphy, Biostratigraphic Series*, 1:29-34.

Lucas, S.J. and Hancox, P.J. 2001. Tetrapod-based correlation of the nonmarine upper Triassic of southern Africa. *Albertiana*, 25:5-9.

Marsh, J.S., Hooper, P.R., Rehacek, J., Duncan, R.A., and Duncan, A.R. 1997. Stratigraphy and age of Karoo Basalts of Lesotho and implications for correlations within the Karoo Igneous Province. *Geophysical Monograph*, 100:247-272.

Marsh, J.S., Swart, R.S., and Phillips, D. 2004. Implications of a new $^{40}Ar/^{39}Ar$ age for a basalt flow interbedded with the Etjo Formation, northeast Namibia. South African *Journal of Geology*, 106: 281-286.

Migeod, F.W.H. 1931. British Museum East Africa Expedition. Account of the work done in 1930. *Natural History Magazine*, 87-103.

Newton, R.B. 1910. Notes on some fossil non –marine Mollusca and a bivalved crustacean (Estheriella) from Nyasaland. *Quarterly Journal of the Geological Society of London*, 66:239-248.

Renne, P.R., Deino, A.L., Walter, R.C., Turrin, B.D., Swisher, C.C., Becker, T.A., Curtis, G.H., Sharp, W.D., and Jaouni, A.-R. 1994. Intercalibration of astronomical and radioisotopic time. *Geology*, 22:783-786.

Rubidge, B.S. (ed.). 1995. Biostratigraphy of the Beaufort Group (Karoo Supergroup). *Geological Survey of South Africa, South African Committee for Stratigraphy, Biostratigraphic Series* 1:1-46.

Rubidge, B.S. and Kitching, J.W. 2003. A new burnetiamorph (Therapsida: Biarmosuchia) from the lower Beaufort Group of South Africa. *Palaeontology*, 46:199-210.

Rubidge, B.S. and Sidor, C.A. 2001. Evolutionary patterns among Permo-Triassic therapsids. *Annual Review of Ecology and Systematics*, 449-480.

Rubidge, B.S. and Sidor, C.A. 2002. On the cranial morphology of the basal therapsids *Burnetia* and *Proburnetia* (Therapsida: Burnetiidae). *Journal of Vertebrate Paleontology*, 22:257-267.

Sandrock, O., Dauphin, Y., Kullmer, O., Abel, R., Schrenk, F., and Denys, C. 1999. Malema: Preliminary taphonomic analysis of an African hominid locality. *Comptes rendus de l-Académie des Sciences Paris, Earth and Planetary Sciences*, 328:133-139.

Schrenk, F., Bromage, T.G., Betzler, C.G., Ring, U., and Juwayeyi, Y.M. 1993. Oldest *Homo* and Pliocene biogeography of the Malawi Rift. *Nature*, 365:833-836.

Sharp, W.D., Turrin, B.D., Renne, P.R., and Lanphere, M.A. 1996. The 40Ar/39Ar and K/Ar dating of lavas from the Hilo 1-km core hole, Hawaii Scientific Drilling Project. *Journal of Geophysical Research*, 101:B5:11607-11616.

Sidor, C.A. 2001. Simplification as a trend in synapsid cranial evolution. *Evolution*, 55:1419-1442.

Sidor, C.A. 2003. The naris and palate of *Lycaenodon longiceps* (Therapsida: Biarmosuchia), with comments on their early evolution in the Therapsida. *Journal of Paleontology*, 77:977-984.

Sidor, C.A. and Hopson, J.A. 1998. Ghost lineages and "mammalness": Assessing the temporal pattern of character acquisition in the Synapsida. *Paleobiology*, 24:254-273.

Sidor, C.A., Hopson, J.A., and Keyser, A.W. 2004. A new burnetiamorph therapsid from the Teekloof Formation, Permian, of South Africa. *Journal of Vertebrate Paleontology*, 24:938-950.

Sidor, C.A. and Welman, J. 2003. A second specimen of *Lemurosaurus pricei* (Therapsida: Burnetiamorpha). *Journal of Vertebrate Paleontology*, 23:631-642.

Sigogneau, D. 1970. *Révision systématique des Gorgonopsiens sud-africains*. Cahiers de Paleontologie, Paris.

Sigogneau-Russell, D. 1989. *Theriodontia I: Pthinosuchia, Biarmosuchia, Eotitanosuchia, Gorgonopsia*. Encyclopedia of Paleoherpetology. Gustav Fischer Verlag, Stuttgart.

Smith, R.M.H. 1990. Alluvial paleosols and pedofacies sequences in the Permian Lower Beaufort of the southwestern Karoo Basin, South Africa. *Journal of Sedimentary Petrology*, 60:258-276.

Smith, R.M.H. 1993. Vertebrate taphonomy of Late Permian floodplain deposits in the southwestern Karoo Basin of South Africa. *Palaios*, 8:45-67.

Smith, R.M.H., Eriksson, P.G., and Botha, W.J. 1993. A review of the stratigraphy and sedimentary environments of the Karoo-aged basins of southern Africa. *Journal of African Earth Sciences*, 16:143-169.

Smith, R.H.M. and Keyser, A.W. 1995a. Biostratigraphy of the *Pristerognathus* Assemblage Zone. *Geological Survey of South Africa, South African Committee for Stratigraphy, Biostratigraphic Series,* 1:13-17.

Smith, R.H.M. and Keyser, A.W. 1995b. Biostratigraphy of the *Tropidostoma* Assemblage Zone. *Geological Survey of South Africa, South African Committee for Stratigraphy, Biostratigraphic Series*, 1:18-22.

Smith, R.H.M. and Keyser, A.W. 1995c. Biostratigraphy of the *Cistecephalus* Assemblage Zone. *Geological Survey of South Africa, South African Committee for Stratigraphy, Biostratigraphic Series*, 1:23-28.

Stollhofen, H., Stanistreet, I.G., Bangert, B., and Grill, H. 2000. Tuffs, tectonism and glacially related sea-level changes, Carboniferous-Permian, southern Namibia. *Palaeogeography, Palaeoclimatology, Palaeoecology*, 161:127-150.

Traquair, R.H. 1910. Notes on fossil-fish remains from Nyasaland collected by Mr. A.R. Andrew and Mr. T.E.G. Bailey. *Quarterly Journal of the Geological Society of London*, 66:249-252.

Turner, B.R. 1999. Tectonostratigraphical development of the upper Karoo foreland basin: Orogenic unloading versus thermally-induced Gondwana Rifting. *Journal of African Earth Sciences*, 28:215-238.

Visser, J.N.J. 1991. Geography and climatology of the late Carboniferous to Jurassic Karoo Basin in southwestern Gondwana. *Annals of the South African Museum*, 99:415-431.

Yemane, K. 1993. Contribution of late Permian palaeogeography in maintaining a temperate climate in Gondwana. *Nature*, 361:51-54.

Yemane, K. 1994. Palynoflora and kerogen constituents of an upper Permian Gondwana deposit, northern Malawi; implications for paleoclimate and source-rock potential. Pangaea: Global environments and resources. *Canadian Society of Petroleum Geologists Memoir,* 17:449-468.

Yemane, K. and Kelts, K. 1990. A short review of palaeoenvironments for lower Beaufort (upper Permian) Karoo sequences from southern to central Africa: A major Gondwana lacustrine episode. *Journal of African Earth Sciences*, 10(1/2):169-185.

Yemane, K. and Kelts, K. 1996. Isotope geochemistry of Upper Permian early diagenetic calcite concretions: Implications for Late Permian waters and surface temperatures in continental Gondwana. *Palaeogeography, Palaeoclimatology, Palaeoecology*, 125:51-73.

Yemane, K., Siegenthaler, C., and Kelts, K. 1989. Lacustrine environment during lower Beaufort (upper Permian) Karoo deposition in northern Malawi. *Palaeogeography, Palaeoclimatology, Palaeoecology*, 70:165-178.

Appendix 1. List of characters (modified from Sidor and Welman 2003) used to construct the cladograms in Figure 10.

1. Premaxillary vomerine processes: short (0), long, bounding vomer in between and approaching level of upper canine posteriorly (1).

2. Length of dorsal process of premaxillae: short (0), or long, reaching to level posterior to that of upper canine (1).

3. Septomaxilla contained within external naris (0) or escaping to facial exposure (1).

4. Lateral surface of lacrimal bearing one or more deep fossae: absent (0), present (1).

5. Maxilla contacting prefrontal: absent (0), present (1).

6. Shape of dorsal surface of nasals: flat (0), with narrow, ridge-like eminence (1), with transversely expanded median boss (2).

7. Supraorbital margin thin (0), moderately thickened (1), or greatly thickened into boss (2).

8. Boss at posterodorsal margin of orbit, near origin of postorbital bar: absent (0), present (1).

9. Ventrolateral surface of zygomatic arch and suborbital bar: smooth (0), or with two ventrolaterally projecting knobs (1).

10. Squamosal thickened on ventral surface of zygomatic arch lateral to position of quadrate: absent (0), present (1).

11. Posterior portion of zygomatic arch bent strongly ventrally: absent (0), present (1).

12. Squamosal "horns" directed posterodorsally from skull roof: absent (0), present (1).

13. Squamosal thickened along its posterior border with tabular: absent (0), present and well developed (1).

14. Shape of dorsal surface of frontals: flat (0), with low ridge (1), or with tall, thickened ridge (2).

15. Length of posterior process of postorbital: stopping above LTF (0), descending onto posterior margin of LTF (1).

16. Circum-pineal parietal shape: flat (0), low and diffuse swelling (1), or forming well-defined chimney (2).

17. Preparietal: absent (0), present (1).

18. Supratemporal: present (0), absent (1).

19. Interchoanal portion of vomer broad (0) or forming median ridge (1) where it meets post-choanal portion.

20. Medial edge of pterygoid basicranial ramus having parasagittal ventral ridge: absent (0), present (1).

21. Row of teeth on transverse flange of pterygoid: present (0), absent (1).

22. Ectopterygoid teeth: present (0), absent (1).

23. Palatine dentition broadly distributed (0), or restricted to small area (1) on palate.

24. Position of transverse flange of pterygoid: under posterior half of orbit (0), under anterior half of orbit (1), or preorbital (2).

25. Basicranial rami of pterygoids broadly separated (0), narrowly separated with median trough formed (1), or broadly contacting anterior to basicranium (2).

26. Forward rotation of occiput: none (0), moderate (5vertical) (1).

27. Stapedial foramen: present (0), absent (1).

28. Exoccipitals meeting (0) or separated (1) on dorsal surface of occipital condyle.

29. Shape of postparietal: wider than tall (0), approximately square (1), or taller than wide (2).

30. Dentary-angular suture shape: diagonal (0), or posterior margin of dentary deeply incised (1).

31. Angular with pattern of ridges and fossae on its lateral surface: absent (0), present (1).

32. Articular dorsal process: absent (0), present (1).

33. Dorsal edge of surangular just posterior to dentary with laterally projecting ridge: absent (0), or present (1).

34. Upper incisors large, approaching size of caniniform tooth (0) or much smaller than caniniforms (1).

35. Upper and lower incisors intermesh: absent (0), present in anterior incisors (1), present in all incisors (2).

36. Lower canine fiting into choana (0), or into fossa roofed by premaxilla and maxilla (1).

37. Number of upper postcanines: 12 or more (0), fewer than 12 (1).

Lab ID#	Watts	Irrad.	J ($\times 10^{-3}$)	$\pm 1\sigma$	^{40}Ar	$\pm 1\sigma$	^{39}Ar	$\pm 1\sigma$	^{38}Ar	$\pm 1\sigma$	^{37}Ar	$\pm 1\sigma$	^{36}Ar	$\pm 1\sigma$	^{39}Ar Mol $\times 10^{-14}$	^{39}Ar % of total	$\%(^{36}Ar)_{Ca}$	Ca/K	$\pm 1\sigma$	$\%^{40}Ar^*$	Age (Ma)	$\pm 1\sigma$	w/$\pm J$ $\pm 1\sigma$
LJ-3																							
4496-01A	0.1	51F	21.80	0.12	0.000	0.017	0.000	0.004	0.000	0.005	0	0	0.001	0.002	0.00	0.0	0.0	0	0	242.1	1669	2825	2825.50
4496-01B	0.2	51F	21.80	0.12	0.32	0.02	0.000	0.004	0.000	0.005	0	0	0.0006	0.0015	0.00	0.0	0.0	0	0	42.6		13765	13765.49
4496-01C	0.3	51F	21.80	0.12	280	2	18.47	0.15	0.629	0.010	5.27	0.06	0.602	0.009	1.94	7.9	0.2	0.559	0.008	36.6	206	7	7.50
4496-01D	0.4	51F	21.80	0.12	309.3	1.6	58.3	0.4	0.743	0.010	15.93	0.13	0.096	0.004	6.13	25.0	4.3	0.536	0.005	91.3	181.0	1.7	1.95
4496-01E	0.5	51F	21.80	0.12	208.1	1.3	42.0	0.3	0.524	0.005	22.7	0.2	0.035	0.002	4.41	18.0	16.9	1.062	0.012	95.9	178.0	1.8	2.00
4496-01F	0.6	51F	21.80	0.12	113.8	1.7	23.1	0.3	0.297	0.006	21.2	0.3	0.0100	0.0010	2.43	9.9	54.9	1.80	0.04	98.8	182	4	3.81
4496-01G	0.8	51F	21.80	0.12	115	2	23.4	0.5	0.345	0.009	32.8	0.7	0.021	0.002	2.46	10.0	39.9	2.74	0.08	96.7	178	5	5.37
4496-01H	1.1	51F	21.80	0.12	80.6	1.4	16.5	0.2	0.266	0.008	31.3	0.4	0.018	0.002	1.73	7.1	43.8	3.73	0.07	96.2	176	4	4.38
4496-01I	1.4	51F	21.80	0.12	51.0	0.5	10.71	0.17	0.193	0.005	22.40	0.16	0.014	0.004	1.13	4.6	42.4	4.10	0.07	95.5	171	5	4.80
4496-01J	1.9	51F	21.80	0.12	65.9	0.8	13.50	0.11	0.249	0.006	37.0	0.5	0.034	0.002	1.42	5.8	28.0	5.37	0.08	89.0	163	3	3.18
4496-01K	2.5	51F	21.80	0.12	39.7	0.3	7.98	0.09	0.131	0.005	33.0	0.3	0.0236	0.0018	0.84	3.4	36.1	8.10	0.11	88.8	167	3	3.40
4496-01L	3.3	51F	21.80	0.12	31.2	0.4	6.02	0.08	0.119	0.004	37.1	0.7	0.033	0.005	0.63	2.6	29.5	12.1	0.3	78.3	154	10	9.63
4496-01M	7.5	51F	21.80	0.12	93.6	0.9	13.48	0.11	0.316	0.006	171.6	1.7	0.165	0.005	1.42	5.8	26.9	25.0	0.3	61.9	163	5	4.80
																100.0		0.681	0.004				
LJ-3 2																							
4496-02A	0.3	51F	21.80	0.12	480	2	29.67	0.18	1.252	0.011	9.51	0.11	1.115	0.006	3.12	5.9	0.2	0.628	0.008	31.5	190	5	5.06
4496-02B	0.4	51F	21.80	0.12	195.8	1.6	29.8	0.3	0.499	0.007	6.84	0.12	0.146	0.004	3.13	5.9	1.2	0.449	0.009	78.3	192	3	3.35
4496-02C	0.4	51F	21.80	0.12	244.8	1.3	44.8	0.3	0.598	0.007	11.59	0.08	0.081	0.003	4.70	8.9	3.7	0.507	0.004	90.6	185.0	1.7	1.96
4496-02D	0.5	51F	21.80	0.12	527.7	1.0	106.0	0.3	1.353	0.011	41.5	0.4	0.0793	0.0011	11.14	21.1	13.5	0.767	0.007	96.2	179.1	0.7	1.20
4496-02E	0.6	51F	21.80	0.12	386.5	1.7	79.28	0.11	1.012	0.010	58.2	0.2	0.041	0.004	8.33	15.7	36.5	1.438	0.006	98.0	178.8	1.0	1.40
4496-02F	0.8	51F	21.80	0.12	259.4	0.3	53.37	0.08	0.66	0.04	70.4	0.4	0.0281	0.0020	5.61	10.6	64.8	2.587	0.015	98.9	179.9	0.6	1.14
4496-02G	1.1	51F	21.80	0.12	198	2	41.1	0.5	0.731	0.010	80.1	0.9	0.036	0.002	4.31	8.2	57.2	3.82	0.06	97.7	176	3	3.07
4496-02H	1.4	51F	21.80	0.12	111.1	1.5	23.7	0.3	0.470	0.008	51.4	0.6	0.020	0.002	2.49	4.7	65.6	4.25	0.07	98.2	173	3	3.49
4496-02I	1.9	51F	21.80	0.12	159.5	1.3	33.76	0.19	0.669	0.009	84.0	0.5	0.0618	0.0018	3.55	6.7	35.1	4.88	0.04	92.6	164.5	1.8	2.03
4496-02J	2.5	51F	21.80	0.12	102.3	1.5	21.1	0.4	0.367	0.008	64.0	1.0	0.046	0.002	2.22	4.2	35.8	5.93	0.14	91.5	167	4	4.21
4496-02K	3.3	51F	21.80	0.12	80.8	1.2	16.4	0.2	0.286	0.007	85.6	1.3	0.055	0.004	1.72	3.3	39.8	10.23	0.20	87.8	163	4	4.32
4496-02L	5.5	51F	21.80	0.12	83.5	1.4	16.4	0.2	0.296	0.007	162	3	0.092	0.004	1.73	3.3	45.4	19.3	0.4	82.2	158	5	4.75
4496-02M	8.0	51F	21.80	0.12	42.4	1.1	8.2	0.2	0.131	0.006	50.8	1.1	0.036	0.003	0.86	1.6	36.1	12.2	0.4	83.8	164	7	7.36
																100.0		0.882	0.003				
LJ-4																							
4494-01A	8.0	51F	21.80	0.12	432	4	29.1	0.6	1.017	0.009	7.89	0.11	0.942	0.005	3.06	7.4	0.2	0.532	0.014	35.8	198	7	7.30
4494-01B	0.4	51F	21.80	0.12	422.8	1.2	82.77	0.15	1.117	0.012	16.93	0.11	0.175	0.003	8.70	21.1	2.5	0.401	0.003	88.1	168.8	0.9	1.24
4494-01C	0.6	51F	21.80	0.12	500.5	1.7	107.2	0.3	1.388	0.009	51.6	0.4	0.090	0.003	11.27	27.4	14.9	0.944	0.007	95.5	167.3	0.9	1.24
4494-01D	0.8	51F	21.80	0.12	200.7	1.4	42.5	0.2	0.587	0.007	47.4	0.3	0.044	0.002	4.46	10.9	27.8	2.189	0.017	95.3	169.0	1.6	1.82
4494-01E	1.1	51F	21.80	0.12	117.5	1.8	23.9	0.4	0.411	0.007	40.1	0.8	0.054	0.002	2.51	6.1	19.1	3.28	0.08	89.0	164	4	3.99
4494-01F	1.4	51F	21.80	0.12	106.1	1.4	20.4	0.2	0.445	0.006	38.4	0.4	0.0702	0.0018	2.14	5.2	14.1	3.69	0.06	83.2	163	3	3.41
4494-01G	1.9	51F	21.80	0.12	192	2	33.4	0.3	0.790	0.010	85.1	1.4	0.212	0.006	3.51	8.5	10.4	4.99	0.09	70.8	154	3	3.46
4494-01H	2.5	51F	21.80	0.12	146.5	1.2	22.7	0.2	0.509	0.008	80.2	1.0	0.1985	0.0013	2.38	5.8	10.4	6.94	0.10	64.2	157	3	2.83
4494-01I	3.3	51F	21.80	0.12	102.7	0.5	16.78	0.04	0.380	0.008	156.8	0.5	0.156	0.003	1.76	4.3	25.9	18.32	0.07	66.7	155	3	2.82
4494-01J	4.8	51F	21.80	0.12	90.8	0.9	12.59	0.18	0.320	0.007	109.1	0.7	0.155	0.003	1.32	3.2	18.2	17.0	0.3	58.8	160	5	4.82
																100.0		0.539	0.002				
LJ-4 2																							
4494-02A	0.1	51F	21.80	0.12	0.04	0.02	0.001	0.006	0.001	0.004	0.0	0.0	0.0000	0.0016	0.00	0.0	0.0	8	110	169.2	1852	11221	11221.11
4494-02B	0.2	51F	21.80	0.12	0.04	0.03	0.000	0.004	0.000	0.005	0.0	0.0	0.000	0.007	0.00	0.0	0.1	4	12	4367.6		0	0.00
4494-02C	0.3	51F	21.80	0.12	181.3	1.0	14.82	0.10	0.436	0.007	4.52	0.08	0.324	0.003	1.56	5.2	0.4	0.598	0.012	47.4	215	4	4.11
4494-02D	0.4	51F	21.80	0.12	264.7	0.8	47.91	0.15	0.648	0.007	11.65	0.07	0.130	0.004	5.03	16.9	2.3	0.477	0.003	85.8	177.5	1.3	1.62
4494-02E	0.5	51F	21.80	0.12	249.5	1.5	53.2	0.2	0.648	0.008	19.62	0.18	0.043	0.002	5.58	18.7	11.8	0.723	0.007	95.5	168.2	1.4	1.66
4494-02F	0.6	51F	21.80	0.12	169.2	1.1	36.59	0.18	0.448	0.007	21.9	0.2	0.0192	0.0008	3.84	12.9	29.4	1.170	0.014	97.6	169.4	1.4	1.69
4494-02G	0.8	51F	21.80	0.12	162.9	1.4	35.2	0.3	0.459	0.006	32.4	0.2	0.0219	0.0019	3.70	12.4	38.3	1.807	0.018	97.6	169	2	2.24
4494-02H	1.1	51F	21.80	0.12	117.1	0.8	25.13	0.18	0.379	0.005	35.9	0.3	0.0196	0.0018	2.64	8.8	47.4	2.80	0.03	97.4	170.3	1.8	2.03

(cont'd)

Lab ID#	Watts	Irrad.	J (X 10⁻³) ±1σ		Relative Isotopic Abundances										Derived Results							
					^{40}Ar ±1σ		^{39}Ar ±1σ		^{38}Ar ±1σ		^{37}Ar ±1σ		^{36}Ar ±1σ		^{39}Ar Mol × 10⁻¹⁴	^{39}Ar % of total	%(^{36}Ar)$_{Ca}$	Ca/K ±1σ		%$^{40}Ar^*$	Age (Ma) ±1σ		w/±J ±1σ
4494-02I	*1.4*	*51F*	*21.80*	*0.12*	*69.0*	*0.7*	*14.69*	*0.12*	*0.269*	*0.006*	*28.2*	*0.4*	*0.018*	*0.002*	*1.54*	*5.2*	*40.3*	*3.76*	*0.06*	*95.4*	*168*	*3*	*2.87*
4494-02J	1.9	51F	21.80	0.12	82.0	0.9	17.10	0.15	0.367	0.007	41.2	0.4	0.040	0.003	1.80	6.0	26.3	4.72	0.06	89.3	161	3	3.10
4494-02K	2.5	51F	21.80	0.12	60.3	0.7	12.28	0.16	0.245	0.006	50.2	0.8	0.050	0.003	1.29	4.3	25.9	8.01	0.17	81.9	152	4	3.84
4494-02L	3.3	51F	21.80	0.12	37.1	0.5	7.21	0.08	0.122	0.006	36.18	0.12	0.039	0.002	0.76	2.5	23.9	9.84	0.11	76.4	149	5	4.83
4494-02M	7.5	51F	21.80	0.12	117.9	1.0	19.86	0.19	0.376	0.007	208.3	1.5	0.188	0.004	2.09	7.0	28.6	20.6	0.2	66.4	150	3	3.35
																100.0		0.621	0.003				

NOTES:

Samples were irradiated for 28.7 hours in the central thimble facility of the now-decommissioned Omega West reactor of the Los Alamos National Laboratories. Sanidine from the Pahranagat Lakes Tuff of Nevada was used as the neutron fluence monitor with a reference age of 22.782 Ma (Best *et al.*, 1995; Renne *et al.*, 1998). Analyses in italics are included in the step-heating age plateau for each sample.

Nucleogenic production ratios:

($^{36}Ar/^{37}Ar)_{Ca}$	2.582	± 0.06	× 10⁻⁴
($^{39}Ar/^{37}Ar)_{Ca}$	6.7	± 0.3	× 10⁻⁴
($^{38}Ar/^{37}Ar)_{Ca}$	1.4		× 10⁻⁴
($^{40}Ar/^{39}Ar)_{K}$	8	± 7	× 10⁻⁴
($^{38}Ar/^{39}Ar)_{K}$	1.077		× 10⁻²
($^{36}Ar/^{38}Ar)_{Cl}$	3.2		× 10²
$^{37}Ar/^{39}Ar$ to Ca/K	1.96		

Isotopic constants and decay rates:

λ($^{40}K_{e}$) /yr	5.81	± 0.17	× 10⁻¹¹
λ($^{40}K_{β-}$) /yr	4.962	± 0.086	× 10⁻¹⁰
λ(^{37}Ar) /d	1.975		× 10⁻²
λ(^{39}Ar) /d	7.068		× 10⁻⁶
λ(^{36}Cl) /d	6.308		× 10⁻⁹
($^{40}Ar/^{36}Ar)_{Atm}$	295.5	± 0.5	
($^{40}Ar/^{38}Ar)_{Atm}$	1575	± 2	
$^{40}K/K_{Total}$	0.01167		

Best, M.G., Christiansen, E.H., Deino, A.L., Grommé, C.S., and Tingey, D.G, 1995, Correlation and emplacement of a large, zoned, discontinuously exposed ash-flow sheet: $^{40}Ar/^{39}Ar$ chronology, paleomagnetism, and petrology of the Pahranagat Formation, Nevada: Jour. Geophys. Res 100:B12:24593–24609.

Renne, P.R., Deino, A.L., Walter, R.C., Turrin, B.D., Swisher, C.C., Becker, T.A., Curtis, G.H., Sharp, W.D., and Jaouni, A-R., 1994, Intercalibration of astronomical and radioisotopic time: Geology 22:783–786.